

Dynamical effects of QCD in $q^2\bar{q}^2$ systems

M. Imran Jamil ^{*}, Bilal Masud [†]

Centre For High Energy Physics, University of the Punjab, Lahore(54590), Pakistan.

Abstract

The dynamical effects of lattice QCD based area-dependant gluon field overlap factor f has been seen in comparison to the Gaussian form. In this comparison it has been found that the phase shifts, in the absence of spin and flavor degrees of freedom, depend upon scattering angle when this multi-body non-separable f is used in off-diagonal elements of potential energy, kinetic energy and normalization matrices of model of $q^2\bar{q}^2$ systems in the gluonic cluster basis. So the lattice-based form of f not only tackle the Van-der-Walls force problem but points certain features (non-separability of f) of QCD that are 1) present in the lattice simulations and 2) can be compared with actual experiments. To write the total state vector of the $q^2\bar{q}^2$ we have used the resonating group method, and decoupled the resulting more complicated integral equations through the Born approximation.

1 Introduction

Models of hadronic physics are to be compared with experimental results as well as with our understanding of QCD for large momentum transfers *and* for low momentum transfers where Feynman diagrams are not useful. In this way, models may help us improving our knowledge of QCD for low and intermediate energies of interest to hadronic spectroscopy and eventually nuclear physics. One way to get this understanding is to note some features present in the perturbative QCD, lattice gauge theory or models of atomic and nuclear physics and check if these features can be used in the low and intermediate energy hadronic physics.

One such feature is an approach based on pair-wise interaction for an interacting multiparticle system (composed of more than two or three particles). This has been successful in atomic and many-nucleon systems; the corresponding two-body interaction being described by Coulombic and Yukawa potential, for example. The question is if the explicit presence of *Non-Abelian* gluon field can also be replaced by *two body* interquark potentials. The simplest way to use such a model is to try a *sum* of two-body potentials or interactions, the usual approach of atomic and nuclear physics. For comparison, it can be noted that the lowest order perturbative Feynman diagrams amplitudes are of this form, and a simple extension of this diagrammatic approach to multi-quarks also has this pattern; see ref. [1], and the later in the same approach, where the one gluon exchange potential, though, is replaced by Coulombic-plus-linear-plus-hyperfine. If the energies of the four-quark systems are numerically calculated, in the static quark limit, on a lattice are compared with models that use only a *sum* of two-quark potentials, the model give a gross overestimate of the (magnitude of) four-quark binding energies; see Fig. 4 of the same ref.[2]. A gluon field overlap factor f was introduced [3] essentially as a solution to this discrepancy. This factor multiplied only off-diagonal elements of the overlap, kinetic and potential energy matrices of the otherwise pairwise-sum-based Hamiltonian in the three-dimensional basis of the model system of four valence quarks/antiquarks and the purely gluonic field between them.

The use of this f factor solves the well known Van der Walls force problem [4] with the otherwise naive sum of one gluon exchange pair-wise interaction. It has been said [5] that quantitatively it is not a serious problem because of the quark-antiquark pair creation and because of the wave function damping of the large distance configurations. Though, there have been lattice calculations [6] partly incorporating both the quark-antiquark pair creation and the meson wave functions and still showing a need for the f

^{*}e mail: mimranjamil@hotmail.com

[†]e mail: bilalmasud@chep.pu.edu.pk

factor, through the present work we want to point out that the dynamical role of the f factor in meson-meson interactions is *not limited* to solving Van der Waals force problem or pointing out [7] otherwise over-binding in certain meson-meson systems. The f factor points certain features (non-separability of f) of QCD that are 1) indicated by lattice simulations and 2) can be compared with actual experiments.

At the time of its first introduction [3], a Gaussian form of $f(\mathbf{r}_1, \mathbf{r}_2, \mathbf{r}_3, \mathbf{r}_4)$ was chosen for computational convenience. In retrospect, it can be noted that this form was a separable *product* of two body terms, each of the form $\exp(-kr_{ij}^2)$. It can be said that the most general form of the Feynman amplitude of the perturbative QCD is a product of two-body interactions (or propagators) and for a two quarks two-antiquarks system, the simplest (diagonal) [8] Wilson loops are a product of the Wilson loops for quark-antiquark time evolutions. But the QCD Wilson loops in general are not limited [8] to this product form, and there is no reason to restrict models of multi-quarks systems to a sum or product of pair-wise interactions. The actual lattice simulations supported a model [9] for the gluon field overlap f in the form $\exp(-kS)$, with S being the minimal area of the surface bounded by the external straight lines connecting the quarks and antiquarks.

This much for a comparison of the f model with lattice simulations; the more refined lattice simulation results [6] were parameterized by a Gaussian form of f for computational convenience, but could be better parameterized by the area form. For a comparison with actual hard experiments, we have to incorporate quark motion as well. Though this has been partly done by lattice unquenched simulations that calculated [6] effects of the motion of two light quarks, models of the multi-quark systems have to include the quark motion through quark wave functions within a single cluster (meson in our case). The resulting four-body Schrödinger equation can be solved, as in ref. [5], variationally for the ground state of the system and the effective meson-meson potentials. Alternatively, the Hamiltonian emerging from the $q^2\bar{q}^2$ model has been diagonalized in the simple harmonic oscillator basis [10], or was sandwiched between the external meson wave functions to give a transition amplitude of the *Born diagrams* [1][11] that is related to meson-meson phase shifts. We have used a method (resonating group method [12]) that was, for the $q^2\bar{q}^2$ system, originally [3] used in a way that partially allowed finding even the external meson wave functions without specifying the functional form of the *inter-cluster* dependence; the cluster being a meson in our case. But for this, as in the resonating group method, dependence on the within-cluster position vector has to be taken from somewhere else. The formalism allows using the best available knowledge of a meson wave function, though a simple Gaussian form for the wave functions and correspondingly a quadratic quark-antiquark potential was used for computational convenience. We have used this same formalism that can be generalized. But because of the additional computational problems due to a totally non-separable exponential of (a negative constant times) area in f , presently we had to pre-specify a plane-wave form of the inter-cluster dependence that is justified through a feeble inter-cluster (meson-meson) interaction noted in previous works [5, 3, 1]; the meson-meson phase shifts resulting from this work are also much less than a radian. Thus at a later stage the coupled integral equations for inter-cluster wave functions are decoupled in this work. This allowed us to numerically calculate the off-diagonal elements as nine-dimensional integrals for the components of the eventual four position 3-vectors; only the overall center-of-mass dependence could be analytically dealt with in a trivial manner. Before this numerically double integration, for the kinetic energy terms we had to differentiate the area in f . The form of area used in the detailed form of the $Q^2\bar{Q}^2$ model, that we take from ref. [9], has square roots of the functions of our position variables. Thus a differentiation of this area form yields in denominators combinations of position variables that become zero somewhere in the ranges of integrations to be later done. On physical grounds, we expect such poles to cancel and maintain finite values for meson properties. But for this first implementation of the area dependence, only for the to-be-differentiated right \sqrt{f} part of the some kinetic energy terms we replaced the area by an approximated quadratic form whose differentiation does not result in negative powers of the position variables.

The introduction of a many-body interaction in the previous form of f (that is noted to be a product of two-body interactions) resulted in a reduced meson-meson interaction. In ref. [3] this reduction was noted as decreased meson-meson phase shifts. The spin and flavor dependence was not incorporated in this first dynamical calculation with the simplest form of f . In now the first dynamical calculation with the lattice-justified form of f we are again started without including the spin and flavor dependence and tried to find out how this information from lattice gauge theory affects the meson-meson phase shifts. (It is to be noted that in a later work [7] spin and flavor were incorporated for a specific system ($K\bar{K}$), and we are working [13] on including spin and flavor dependence with some different form of f or initially for a different system.)

In section 2 we have written the total state vector of the $q^2\bar{q}^2$ system using the RGM, along with

introducing the Hamiltonian H of the system without the f factor and then modifying H through the f . In section 3 different position dependent forms of f has been described, including the approximate forms that we had to use. In section 4 we have solved the integral equations for a meson meson molecule in the absence of color and flavor degrees of freedom, resulting in a prescription to find the phase shifts. In the last section we have presented the numerical values of the phase shifts for different forms of f , for different values of free parameter k_f and for different values of angle θ between \mathbf{P}_1 and \mathbf{P}_2 .

2 Resonating Group Method (RGM) and the $Q^2\bar{Q}^2$ Hamiltonian

Using adiabatic approximation we can write the total state vector of a system containing two quarks two antiquarks and the gluonic field between them as a sum of product of quarks (Q or \bar{Q}) position dependence function $\Psi_g(\mathbf{r}_1, \mathbf{r}_2, \mathbf{r}_3, \mathbf{r}_4)$ and the gluonic field state $|k\rangle_g$. $|k\rangle_g$ is defined as a state which approaches $|k\rangle_c$ in the weak coupling limit, with $|1\rangle_c = |1_{1\bar{3}}1_{2\bar{4}}\rangle_c$, $|2\rangle_c = |1_{1\bar{4}}1_{2\bar{3}}\rangle_c$ and $|3\rangle_c = |3_{12}3_{\bar{3}\bar{4}}\rangle_c$. In lattice simulations of the corresponding (gluonic) Wilson loops it is found that the lowest eigenvalue of the Wilson matrix, that is energy of the lowest state, is always the same for both 2×2 and 3×3 matrices provided that $|1\rangle_g$ or $|2\rangle_g$ has the lowest energy [9]. Taking advantage of this observation, we have included in our expansion only two basis states. Using resonating group method $\Psi_g(\mathbf{r}_1, \mathbf{r}_2, \mathbf{r}_3, \mathbf{r}_4)$ or $\Psi_g(\mathbf{R}_c, \mathbf{R}_k, \mathbf{y}_k, \mathbf{z}_k)$ can be written as product of known dependence on $\mathbf{R}_c, \mathbf{y}_k, \mathbf{z}_k$ and unknown dependence on \mathbf{R}_k . i.e. $\Psi_g(\mathbf{r}_1, \mathbf{r}_2, \mathbf{r}_3, \mathbf{r}_4) = \Psi_c(\mathbf{R}_c)\chi_k(\mathbf{R}_k)\psi_k(\mathbf{y}_k, \mathbf{z}_k)$. Here \mathbf{R}_c is the center of mass coordinate of the whole system, \mathbf{R}_1 is the vector joining the center of mass of the clusters $(1, \bar{3})$ and $(2, \bar{4})$, \mathbf{y}_1 is the position vector of quark 1 with respect to $\bar{3}$ within the cluster $(1, \bar{3})$ and \mathbf{z}_1 is the position vector of quark 2 with respect to $\bar{4}$ within the cluster $(2, \bar{4})$. The same applies to $\mathbf{R}_2, \mathbf{y}_2$ and \mathbf{z}_2 for the clusters $(1, \bar{4})$ and $(2, \bar{3})$. Similarly we can define $\mathbf{R}_3, \mathbf{y}_3$ and \mathbf{z}_3 for the clusters $(1, 2)$ and $(\bar{3}, \bar{4})$. Or we can write them in terms of position vector of four quarks/antiquarks as follow

$$\mathbf{R}_1 = \frac{1}{2}(\mathbf{r}_1 + \mathbf{r}_{\bar{3}} - \mathbf{r}_2 - \mathbf{r}_{\bar{4}}), \mathbf{y}_1 = \mathbf{r}_1 - \mathbf{r}_{\bar{3}} \text{ and } \mathbf{z}_1 = \mathbf{r}_2 - \mathbf{r}_{\bar{4}}, \quad (1)$$

$$\mathbf{R}_2 = \frac{1}{2}(\mathbf{r}_1 + \mathbf{r}_{\bar{4}} - \mathbf{r}_2 - \mathbf{r}_{\bar{3}}), \mathbf{y}_2 = \mathbf{r}_1 - \mathbf{r}_{\bar{4}} \text{ and } \mathbf{z}_2 = \mathbf{r}_2 - \mathbf{r}_{\bar{3}} \quad (2)$$

and

$$\mathbf{R}_3 = \frac{1}{2}(\mathbf{r}_1 + \mathbf{r}_2 - \mathbf{r}_{\bar{3}} - \mathbf{r}_{\bar{4}}), \mathbf{y}_3 = \mathbf{r}_1 - \mathbf{r}_2 \text{ and } \mathbf{z}_3 = \mathbf{r}_{\bar{3}} - \mathbf{r}_{\bar{4}}. \quad (3)$$

Thus meson meson state vector in the restricted gluonic basis is

$$|\Psi(\mathbf{r}_1, \mathbf{r}_2, \mathbf{r}_3, \mathbf{r}_4; g)\rangle = \sum_{k=1}^2 |k\rangle_g \Psi_c(\mathbf{R}_c)\chi_k(\mathbf{R}_k)\xi_k(\mathbf{y}_k)\zeta_k(\mathbf{z}_k). \quad (4)$$

Here $\xi_k(\mathbf{y}_k) = \frac{1}{(2\pi d^2)^{\frac{3}{4}}} \text{Exp}[\frac{-\mathbf{y}_k^2}{4d^2}]$ and $\zeta_k(\mathbf{z}_k) = \frac{1}{(2\pi d^2)^{\frac{3}{4}}} \text{Exp}[\frac{-\mathbf{z}_k^2}{4d^2}]$, with the radius of the meson $d = 0.558\text{fm}$ defined by the relation $d^2 = \frac{\sqrt{3}R_c^2}{2}$ [7]. Here $R_c = 0.6\text{fm}$ is the r.m.s. charge radius of the qqq system whose wave function is derived by using the same quadratic confining potential; for numerical convenience, we use a quadratic confining potential.

For $f=1$, the total Hamiltonian H of our 4-particle system is taken as [14]

$$\hat{H} = \sum_{i=1}^4 [m_i + \frac{\hat{P}_i^2}{2m_i}] + \sum_{i<j} v(\mathbf{r}_{ij})\mathbf{F}_i \cdot \mathbf{F}_j. \quad (5)$$

Our same constituent quark mass value $m = 0.3\text{GeV}$ for all quarks and antiquarks is one used in ref. [3], and our kinetic energy operator is similarly non-relativistic; it is included in our aims to compare with this work and isolate the effects only due to a different expression for the f . In above, $F_i = \frac{\lambda_i}{2}$, $i = 1, 2, 3, \dots, 8$, λ_i are Gell-Mann matrices, and

$$v_{ij} = Cr_{ij}^2 + \bar{C} \text{ with } i, j = 1, 2, \bar{3}, \bar{4}. \quad (6)$$

The $q\bar{q}$ potential we use for dynamical calculation is the same as that in ref. [3]. $\xi_k(\mathbf{y}_k)$ and $\zeta_k(\mathbf{z}_k)$ are the normalized eigenfunctions of the $Q\bar{Q}$ Hamiltonian *within* a cluster (unmodified by the f factor). For

this central simple harmonic oscillator potential, the sizes in the eigenfunctions $\xi_k(\mathbf{y}_k)$ and $\zeta_k(\mathbf{z}_k)$ are related to the quadratic coefficient C which thus is given a value of -0.0097GeV^3 ; the choice for \bar{C} value is mentioned below.

Using RGM we take only variations in the χ_k factor of the total state vector of the system. Setting the coefficients of linearly independent arbitrary variations $\delta\chi_k(\mathbf{R}_k)$ as zero and integrating out R_c , $\langle\delta\psi | H - E_c | \psi\rangle = 0$ from eq.(4) gives

$$\sum_{l=1}^2 \int d^3y_k d^3z_k \xi_k(\mathbf{y}_k) \zeta_k(\mathbf{z}_k)_g \langle k | H - E_c | l \rangle_g \chi_l(\mathbf{R}_l) \xi_l(\mathbf{y}_l) \zeta_l(\mathbf{z}_l) = 0, \quad (7)$$

for each of the k values (1 and 2). According to the (2 dimensional basis) model I_a of ref. [9], the normalization, potential energy and kinetic energy matrices in the corresponding gluonic basis are

$$N = \begin{pmatrix} 1 & \frac{1}{3}f \\ \frac{1}{3}f & 1 \end{pmatrix}, \quad (8)$$

$$V = \begin{pmatrix} \frac{-4}{3}(v_{1\bar{3}} + v_{2\bar{4}}) & \frac{4}{9}f(v_{12} + v_{3\bar{4}} - v_{1\bar{3}} - v_{2\bar{4}} - v_{1\bar{4}} - v_{2\bar{3}}) \\ \frac{4}{9}f(v_{12} + v_{3\bar{4}} - v_{1\bar{3}} - v_{2\bar{4}} - v_{1\bar{4}} - v_{2\bar{3}}) & \frac{-4}{3}(v_{1\bar{4}} + v_{2\bar{3}}) \end{pmatrix} \quad (9)$$

and

$${}_g\langle k | K | l \rangle_g = N(f)^{\frac{1}{2}}_{k,l} \left(\sum_{l=1} - \frac{\nabla_l^2}{2m} \right) N(f)^{\frac{1}{2}}_{k,l}. \quad (10)$$

This is the modification, through the f factor, to the Hamiltonian as much as we need it for the integral equations below in section 4 (that is only the modified matrix elements).

3 Different Forms of f

Ref. [9] supports through a comparison with numerical lattice simulations a form f that was earlier [4] suggested through a quark-string model extracted from the strong coupling lattice Hamiltonian gauge theory. This is

$$f = \text{Exp}[-b_s k_f S], \quad (11)$$

S being the area of minimal surface bounded by external lines joining the position of the two quarks and two antiquarks, and $b_s = 0.18\text{GeV}^2$ is the standard string tension [15], k_f is a dimensionless parameter whose value of 0.57 was decided in ref. [9] by a fit of the simplest two-state area-based model (termed model Ia) to the numerical results for a selection of $Q^2\bar{Q}^2$ geometries. It is shown there [9] that the parameters, including k_f , extracted at this SU(2) lattice simulation with $\beta = 2.4$ can be used directly in, for example, a resonating group calculation of a four quark model as the continuum limit is achieved for this value of β .

The simulations reported in ref. [9] were done in the 2-color approximation. But, for calculating the dynamical effects, we use actual SU(3) color matrix elements of ref. [3]. The only information we take from the computer simulations of ref. [9] is value of k_f . This describes a geometrical property of the gluonic field (its spatial rate of decrease to zero) and it may be the case that the geometrical properties of the gluonic field are not much different for different number of colors, as suggested for example by successes of the geometrical flux tube model. Situation is more clear, though, for the mass spectra and the string tension generated by the gluonic field: ref. [16] compare these quantities for SU(2), SU(3) and SU(4) gauge theories in 2+1 dimensions and find that the ratio of masses are, to a first approximation, are independent of the number of colors. Their preliminary calculations in 3+1 dimensions indicate a similar trend. Directly for the parameter k_f , appearing in the overlap factor f studied in this work, a conclusion can be drawn from above mentioned lattice calculations [6] on the interaction energy of the two heavy-light $Q^2\bar{q}^2$ mesons in the realistic SU(3) gauge theory. For interpreting the results in terms of the potential for the corresponding single heavy-light meson ($Q\bar{q}$), a Gaussian form

$$f = \text{Exp}[-b_s k_f \sum_{i<j} r_{ij}^2] \quad (12)$$

of the gluonic field overlap factor f is used in this ref. [6] for numerical convenience and not the minimal area form. But for a particular geometry, the two exponents (the minimal area and the sum of squared distances) in these two forms of f are related and thus for a particular geometry a comparison of the parameter k_f multiplying area and corresponding (different!) k_f multiplying in eq. (14) of a ref. [6] sum of squared is possible. We note that, after correcting for a ratio of 8 between the sum of distance squares (including two diagonals) and the area for the square geometry, the color-number-generated relative difference for this geometry is just 5%: the coefficient is $0.075 \times 8 = 0.6$ multiplying sum of squared distances and 0.57 multiplying the minimal area.

For the area as well, ref. [9] used an approximation: A good model of area of the minimal surface could be that given in ref. [17] as

$$S = \int_0^1 du \int_0^1 dv |(u\mathbf{r}_{1\bar{3}} + (1-u)\mathbf{r}_{\bar{4}2}) \times (v\mathbf{r}_{2\bar{3}} + (1-v)\mathbf{r}_{\bar{4}1})|.$$

(Work is in progress [18], to judge this area/surface model from the point of differential geometry and there are indications that this is quite close to the actual minimal area.) But the simulations reported in ref. [9] were carried out for the S in eq.(11) being "the average of the sum of the four triangular areas defined by the positions of the four quarks". Although for the tetrahedral geometry the S used in ref. [9] is as much as 26 percent larger than the corresponding minimal-like area of ref. [17], it can be expected that their fitted value of k_f is reduced to partially compensate this over estimate of the S area. Anyway, as we are calculating the dynamical effects of the model of ref. [9], we have used the form of S that is used in this work.

The area S of ref. [9] becomes (with a slight renaming)

$S = \frac{1}{2}[S(134) + S(234) + S(123) + S(124)]$, where $S(ijk)$ is the area of the triangle joining the vertices of the positions of the quarks labeled as i,j and k. In the notation of eqs.(1-3) this becomes $S(123) = \frac{1}{2}|\mathbf{y}_3 \times \mathbf{z}_2| = \frac{1}{2}|(\mathbf{R}_1 + \mathbf{R}_2) \times (\mathbf{R}_3 - \mathbf{R}_1)|$, $S(124) = \frac{1}{2}|\mathbf{y}_3 \times \mathbf{z}_1| = \frac{1}{2}|(\mathbf{R}_1 + \mathbf{R}_2) \times (\mathbf{R}_3 - \mathbf{R}_2)|$ etc. Written in terms of the rectangular components (x_1, y_1, z_1) of \mathbf{R}_1 , (x_2, y_2, z_2) of \mathbf{R}_2 and (x_3, y_3, z_3) of \mathbf{R}_3 , this becomes

$$\begin{aligned} S = \frac{1}{4} & \left[\{(x_2^2 + y_2^2 + z_2^2 + 2(x_2x_3 + y_2y_3 + z_2z_3) + x_3^2 + y_3^2 + z_3^2) \right. \\ & \quad \left. (x_1^2 + y_1^2 + z_1^2 - 2(x_1x_2 + y_1y_2 + z_1z_2) + x_2^2 + y_2^2 + z_2^2) \right. \\ & \quad \left. - (x_1x_2 + y_1y_2 + z_1z_2 - (x_2^2 + y_2^2 + z_2^2) + x_1x_3 + y_1y_3 + z_1z_3 - (x_2x_3 + y_2y_3 + z_2z_3))\}^{\frac{1}{2}} + \right. \\ & \quad \left\{ (x_1^2 + y_1^2 + z_1^2 - 2(x_1x_2 + y_1y_2 + z_1z_2) + x_2^2 + y_2^2 + z_2^2) \right. \\ & \quad \left. (x_3^2 + y_3^2 + z_3^2 - 2(x_1x_3 + y_1y_3 + z_1z_3) + x_1^2 + y_1^2 + z_1^2) \right. \\ & \quad \left. - (x_1x_3 + y_1y_3 + z_1z_3 - (x_1^2 + y_1^2 + z_1^2) - (x_2x_3 + y_2y_3 + z_2z_3) + x_1x_2 + y_1y_2 + z_1z_2) \right\}^{\frac{1}{2}} + \\ & \quad \left\{ (x_1^2 + y_1^2 + z_1^2 + 2(x_1x_2 + y_1y_2 + z_1z_2) + x_2^2 + y_2^2 + z_2^2) \right. \\ & \quad \left. (x_3^2 + y_3^2 + z_3^2 - 2(x_1x_3 + y_1y_3 + z_1z_3) + x_1^2 + y_1^2 + z_1^2) \right. \\ & \quad \left. - (x_1x_3 + y_1y_3 + z_1z_3 - (x_1^2 + y_1^2 + z_1^2) + x_2x_3 + y_2y_3 + z_2z_3 - (x_1x_2 + y_1y_2 + z_1z_2)) \right\}^{\frac{1}{2}} + \\ & \quad \left\{ (x_1^2 + y_1^2 + z_1^2 + 2(x_1x_2 + y_1y_2 + z_1z_2) + x_2^2 + y_2^2 + z_2^2) \right. \\ & \quad \left. (x_3^2 + y_3^2 + z_3^2 - 2(x_2x_3 + y_2y_3 + z_2z_3) + x_2^2 + y_2^2 + z_2^2) \right. \\ & \quad \left. - (x_1x_3 + y_1y_3 + z_1z_3 - (x_2^2 + y_2^2 + z_2^2) + x_2x_3 + y_2y_3 + z_2z_3 - (x_1x_2 + y_1y_2 + z_1z_2)) \right\}^{\frac{1}{2}} \Big] \quad (13) \end{aligned}$$

This form of S has square roots. For the $K.E.$ part of the Hamiltonian matrix (see eq.(10)), we have to differentiate an exponential of this square root. After differentiating we can have negative powers of S and when they will be integrated in the latter stages can have singularities in the integrands. To be ready to face this situation in the section below, we have availed to ourselves an approximated S , named S_a , which is a sum of different quadratic combinations of quarks positions. We chose S_a by minimizing $\int (S - S_a)^2 d^3R_1 d^3R_2 d^3R_3$ with respect to the coefficients of the quadratic position combinations; that is, these coefficients are treated as variational parameters. The first (successful) form which we tried for S_a was

$$\begin{aligned} S_a = & a(x_1^2 + y_1^2 + z_1^2) + b(x_2^2 + y_2^2 + z_2^2) + c(x_3^2 + y_3^2 + z_3^2) + d x_1 x_2 + \\ & e y_1 y_2 + f z_1 z_2 + g x_2 x_3 + h y_2 y_3 + i z_2 z_3 + j x_1 x_3 + k y_1 y_3 + l z_1 z_3. \end{aligned} \quad (14)$$

This contained 12 variational parameters a,b,c,...,l. Minimization gave values (reported with accuracy 4

though in the computer program accuracy 16 was used) as

$$a = 0.4065, b = 0.4050, c = 0.3931, j = -0.0002, l = -0.0002.$$

In the reported accuracy other parameters are zero. Here limits of integration were from -15 to 15 in GeV^{-1} . We also tried S_a as

$$\sum_{i=1}^3 a_i(x_i^2 + y_i^2 + z_i^2) + \sum_{i,j=1}^3 (b_{i,j}x_iy_j + c_{i,j}x_iz_j + d_{i,j}y_iz_j) + \sum_{i<j,j=2}^3 (e_{i,j}x_ix_j + f_{i,j}y_iy_j + g_{i,j}z_iz_j)$$

and

$$\sum_{i=1}^3 (l_i x_i^2 + m_i y_i^2 + n_i z_i^2) + \sum_{i,j=1}^3 (b_{i,j}x_iy_j + c_{i,j}x_iz_j + d_{i,j}y_iz_j) + \sum_{i<j,j=2}^3 (e_{i,j}x_ix_j + f_{i,j}y_iy_j + g_{i,j}z_iz_j),$$

with variational parameters being 39 and 45 respectively. Both the latter forms gave the same result as we got with 12 variational parameters, and hence this 12 parameter form was used in the section below. This form gives dimensionless standard-deviation, defined as $\sqrt{\frac{\langle (S-S_a)^2 \rangle - \langle S-S_a \rangle^2}{\langle S^2 \rangle}}$, being approximately equal to 21% . Here, $\langle X \rangle = \frac{\int(X)d^3R_1d^3R_2d^3R_3}{\int(1)d^3R_1d^3R_2d^3R_3}$. As this is not too small, in our main calculations we have made a minimal of this further approximated area S_a (only for the to-be-differentiated right \sqrt{f} part (see eq.10) of the kinetic energy term and here only for derivatives of the exponent).

4 Solving the Integral Equations

In eq.(7) for $k = l = 1$ (a diagonal term), we used the linear independence of $\mathbf{y}_1, \mathbf{z}_1$ and \mathbf{R}_1 (see eq.(1)) to take $\chi_1(\mathbf{R}_1)$ outside the integrations w.r.t. \mathbf{y}_1 and \mathbf{z}_1 . For the off-diagonal term with $k = 1$ we replaced \mathbf{y}_1 and \mathbf{z}_1 with \mathbf{R}_2 and \mathbf{R}_3 , with Jacobian of transformation as 8. For regulating the space derivatives of the exponent of f (see the three sentences immediately following eq.(13) above) we temporarily replaced S in it by its quadratic approximation S_a . As a result, we obtained the following equation:

$$\begin{aligned} & \left(\frac{3\omega}{2} - \frac{1}{2\mu_{12}} \nabla_{R_1}^2 + 24C_o d^2 - \frac{8\bar{C}}{3} - E_c + 4m \right) \chi_1(\mathbf{R}_1) + \\ & \int d^3R_2 d^3R_3 \text{Exp} \left\{ - \left(\frac{R_1^2 + R_2^2 + 2R_3^2}{2d^2} \right) \right\} \text{Exp}(-b_s k_f S) \left[- \frac{8}{6m(2\pi d^2)^3} g_1 \text{Exp} \left(\frac{1}{2} b_s k_f S \right) \text{Exp} \left(- \frac{1}{2} b_s k_f S_a \right) \right. \\ & \left. + \frac{32}{9(2\pi d^2)^3} (-4CR_3^2 - 2\bar{C}) - \frac{8(E_c - 4m)}{3(2\pi d^2)^3} \right] \chi_2(\mathbf{R}_2) = 0, \end{aligned} \quad (15)$$

with, written up to accuracy 4,

$$\begin{aligned} g_1 = & -1.4417 + 0.0258x_1^2 + 0.0258x_2^2 + 0.0254x_3^2 + 0.0258y_1^2 + \\ & 0.0258y_2^2 + 0.0254y_3^2 + 0.0258z_1^2 + 0.0258z_2^2 + 0.0254z_3^2. \end{aligned} \quad (16)$$

For the consistency of $\xi_k(\mathbf{y}_k)$ and $\zeta_k(\mathbf{z}_k)$ with eq.(6) $\omega = \frac{1}{md^2} = 0.416\text{GeV}$. For convenience in notation we take $C_o = -\frac{1}{3}C$. Here in the first channel for $k = 1$ the constituent quark masses has been replaced by the reduced mass $\mu_{12} = \frac{M_1 M_2}{M_1 + M_2}$, where M_1 and M_2 are masses of hypothetical mesons; a similar replacement has been done in ref.[3].

At this stage we can fit \bar{C} to a kind of "hadron spectroscopy" for our flavorless case:

For the large separation there is no interaction between M_1 and M_2 . So the total center of mass energy in the large separation limit will be the sum of kinetic energy of relative motion and masses of M_1 and M_2 i.e. in the limit $R_1 \rightarrow \infty$ we have

$$\left[-\frac{1}{2\mu_{12}} \nabla_{R_1}^2 + M_1 + M_2 \right] \chi_1(\mathbf{R}_1) = E_c \chi_1(\mathbf{R}_1). \quad (17)$$

By comparing, in this limit, eq.(17) and eq.(15) we have $M_1 + M_2 = 4m + 3\omega - \frac{8}{3}\bar{C}$. (A use of the first term of eq.(6) for the color-basis diagonal matrix element of eq.(5) gives $\frac{-4}{3}C = \frac{1}{2}\mu\omega^2 = \frac{1}{2}\frac{\mu\omega}{md^2}$,

giving $24C_0d^2 = \frac{3}{2}\omega$ for the reduced mass μ of a pair of equal mass quarks being $\frac{m}{2}$; the diagonal elements in any form of the f model for the gluonic basis are the same as those for the color basis.) By choosing $M_1 + M_2 = 3\omega$ we have $\bar{C} = \frac{3m}{2} = 0.45\text{GeV}$. This choice of the hypothetical meson masses is the one frequently used in ref. [3] for an illustration of the formalism; when we incorporate flavor and spin dependence [13] the same fit, something like in ref. [7], would be to actual meson spectroscopy. We can then choose to fit even the parameter C or C_0 of our potential model to hadron spectroscopy rather than deciding it, as in ref. [3] and the present work, through a combination of baryon radii and harmonic oscillator model. But we do not see any reason why the qualitative effects (for example, an angle dependence, see the section below) pointed out through the present work should disappear for a phenomenologically explicit case.

Completing our integral equations before finding a solution for two χ' s, for $k = 2$ in eq.(7) we took $\chi_2(\mathbf{R}_2)$ outside of integration for the diagonal term, for the off-diagonal term we replaced \mathbf{y}_2 and \mathbf{z}_2 by \mathbf{R}_1 and \mathbf{R}_3 and replaced S by S_a . This resulted in

$$\begin{aligned} & \left(\frac{3\omega}{2} - \frac{1}{2\mu_{34}} \nabla_{R_2}^2 + 24C_0d^2 - \frac{8}{3}\bar{C} - E_c + 4m \right) \chi_2(\mathbf{R}_2) + \\ & \int d^3R_1 d^3R_3 \text{Exp}\left\{ -\left(\frac{R_1^2 + R_2^2 + 2R_3^2}{2d^2} \right) \right\} \text{Exp}(-b_s k_f S) \left[-\frac{8}{6m(2\pi d^2)^3} g_1 \text{Exp}\left(\frac{1}{2} b_s k_f S \right) \text{Exp}\left(-\frac{1}{2} b_s k_f S_a \right) \right. \\ & \left. + \frac{32}{9(2\pi d^2)^3} (-4CR_3^2 - 2\bar{C}) - \frac{8(E_c - 4m)}{3(2\pi d^2)^3} \right] \chi_1(\mathbf{R}_1) = 0. \end{aligned} \quad (18)$$

In the 2nd channel, for $k = 2$, the constituent quark masses are replaced by the reduced mass $\mu_{34} = \frac{M_3 M_4}{M_3 + M_4}$, where M_3 and M_4 are masses of hypothetical mesons.

Now we solve our two integral equations. As our space derivatives have been regularized, we no longer need further-approximated S_a and we replace this by the original S . Below we take Fourier transform of eq.(15). This gives us a nine dimensional integral of, amongst others, $\text{Exp}(-b_s k_f S)$. Non-separability of S did not allow us to formally solve the two integral equations for a non-trivial solution for χ_1 and χ_2 as in ref. [3] and we had to pre-specify a form for $\chi_2(\mathbf{R}_2)$ in eq.(15) and of $\chi_1(\mathbf{R}_1)$ in eq.(18). Using Born approximation (something already in use [1] for meson-meson scattering; our numerical results mentioned below also justify its use here) we used the solutions of eqs.(15) and (18) in absence of interactions (say by letting k_f approach to infinity, meaning $f = 0$) for $\chi_1(\mathbf{R}_1)$ and $\chi_2(\mathbf{R}_2)$. We chose the coefficient of these plane wave solutions so as to make $\chi_1(\mathbf{R}_1)$ as Fourier transform of $\delta(\frac{P_1 - P_c(1)}{P_c^2(1)})$ and $\chi_2(\mathbf{R}_2)$ as Fourier transform of $\delta(\frac{P_2 - P_c(2)}{P_c^2(2)})$, with $P_c(1)$ and $P_c(2)$ defined below just after eq.(24). Thus we used

$$\chi_2(\mathbf{R}_2) = \sqrt{\frac{2}{\pi}} \text{Exp}(\iota \mathbf{P}_2 \cdot \mathbf{R}_2) \quad (19)$$

inside the integral to get one equation (after the Fourier transform) as

$$\begin{aligned} (3\omega + \frac{P_1^2}{2\mu_{12}} - E_C) \chi_1(\mathbf{P}_1) = & -\sqrt{\frac{2}{\pi}} \frac{1}{(2\pi)^{\frac{3}{2}}} \int d^3R_1 d^3R_2 d^3R_3 \\ & \text{Exp}\{\iota(\mathbf{P}_1 \cdot \mathbf{R}_1 + \mathbf{P}_2 \cdot \mathbf{R}_2)\} \text{Exp}\left\{ -\left(\frac{R_1^2 + R_2^2 + 2R_3^2}{2d^2} \right) \right\} \\ & \text{Exp}(-b_s k_f S) \left[-\frac{8}{6m(2\pi d^2)^3} g_1 + \frac{32}{9(2\pi d^2)^3} (-4CR_3^2 - 2\bar{C}) - \frac{8(E_C - 4m)}{3(2\pi d^2)^3} \right], \end{aligned} \quad (20)$$

with $\chi_1(\mathbf{P}_1)$ being Fourier transform of $\chi_1(\mathbf{R}_1)$. The formal solution [3] of eq.(20) can be written as

$$\begin{aligned} \chi_1(\mathbf{P}_1) = & \delta\left(\frac{P_1 - P_c(1)}{P_c^2(1)} \right) - \frac{1}{\Delta_1(P_1)} \frac{1}{16\pi^5 d^6} \int d^3R_1 d^3R_2 d^3R_3 \text{Exp}\{\iota(\mathbf{P}_1 \cdot \mathbf{R}_1 + \mathbf{P}_2 \cdot \mathbf{R}_2)\} \\ & \text{Exp}\left\{ -\left(\frac{R_1^2 + R_2^2 + 2R_3^2}{2d^2} \right) \right\} \text{Exp}(-b_s k_f S) \left[-\frac{8}{6m} g_1 + \frac{32}{9} (-4CR_3^2 - 2\bar{C}) - \frac{8}{3} (E_C - 4m) \right], \end{aligned} \quad (21)$$

with $\Delta_1(P_1) = \frac{P_1^2}{2\mu_{12}} + 3\omega - E_c - \iota\varepsilon$.

If we choose x -axis along \mathbf{P}_1 and choose z -axis in such a way that xz -plane becomes the plane containing \mathbf{P}_1 and \mathbf{P}_2 , the above equation becomes

$$\chi_1(\mathbf{P}_1) = \delta\left(\frac{P_1 - P_c(1)}{P_c^2(1)} \right) - \frac{1}{\Delta_1(P_1)} \frac{1}{16\pi^5 d^6} F_1, \quad (22)$$

where, in the notation of eq.(13),

$$F_1 = \int_{-\infty}^{\infty} dx_1 dx_2 dx_3 dy_1 dy_2 dy_3 dz_1 dz_2 dz_3 \text{Exp}\{\iota P(x_1 + x_2 \cos\theta + z_2 \sin\theta)\} \text{Exp}(-b_s k_f S) \\ \text{Exp}\left\{-\left(\frac{x_1^2 + y_1^2 + z_1^2 + x_2^2 + y_2^2 + z_2^2 + 2(x_3^2 + y_3^2 + z_3^2)}{2d^2}\right)\right\} \\ \left[-\frac{8}{6m}g_1 + \frac{32}{9}\{-4C(x_3^2 + y_3^2 + z_3^2) - 2\overline{C}\} - \frac{8}{3}(E_C - 4m)\right]. \quad (23)$$

Here θ is the angle between \mathbf{P}_2 and \mathbf{P}_1 and because of elastic scattering $P_1 = P_2 = P$. From eq.(22) we can write, as in ref. [3], the 1, 2 element of the T-matrix as

$$T_{12} = 2\mu_{12}\frac{\pi}{2}P_c F_1. \quad (24)$$

Here $P_c = P_c(2) = P_c(1) = \sqrt{2\mu_{12}(E_c - (M_1 + M_2))}$ and $M_1 = M_2 = \frac{3}{2}\omega$; see paragraph after eq.(17). Using the relation $s = I - 2\iota T = \text{Exp}(2\iota\Delta)$ or $\begin{pmatrix} 1 & 0 \\ 0 & 1 \end{pmatrix} - 2\iota \begin{pmatrix} T_{11} & T_{12} \\ T_{21} & T_{22} \end{pmatrix} = \begin{pmatrix} 1 & 0 \\ 0 & 1 \end{pmatrix} + 2\iota \begin{pmatrix} \delta_{11} & \delta_{12} \\ \delta_{21} & \delta_{22} \end{pmatrix}$ between s matrix and the T matrix (actually in the form of elements $\delta_{ij} = -T_{ij}$ for $i, j = 1, 2$) we got different results for phase shifts for different values of center of mass kinetic energy T_c and the angle θ between \mathbf{P}_1 and \mathbf{P}_2 ; we also probed different values of the parameter k_f .

For a comparison, we also did the much less time consuming (but approximate) calculation using S_a in place of S in eq.(20). This allowed us separating the 9 variables dependence of the integrand as a product, resulting in three triple integrals to be only multiplied, making the convergence very fast in the numerical computation of the integral. Thus we had instead

$$\chi_1(\mathbf{P}_1) = \delta\left(\frac{P_1 - P_c(1)}{P_c^2(1)}\right) - \frac{1}{\Delta_1(P_1)}F, \quad \text{with} \quad (25)$$

$$F = \frac{1}{16\pi^5 d^6} \left[\int_{-\infty}^{\infty} dx_1 dx_2 dx_3 \left\{ \left[-\frac{8}{6m} \right. \right. \right. \\ \left. \left. \left. (-1.4417 + 0.0258x_1^2 + 0.0254x_2^2 - 4.1914 \times 10^{-7}x_1x_3 + 0.0258x_3^2) + \right. \right. \right. \\ \left. \left. \left. \frac{32}{9}(-4Cx_3^2 - 2\overline{C}) - \frac{8}{3}(E_C - 4m) \right\} \text{Exp}\left[-\frac{(x_1^2 + x_2^2 + 2x_3^2)}{2d^2}\right] \right. \right. \\ \left. \left. - b_s k_f (ax_1^2 + dx_1x_2 + jx_1x_3 + bx_2^2 + gx_2x_3 + cx_3^2) \right. \right. \\ \left. \left. + \iota P(x_1 + x_2 \cos\theta) \right] \text{inty} \times \text{intz} + \int_{-\infty}^{\infty} dy_1 dy_2 dy_3 \left\{ \left[-\frac{8}{6m} \right. \right. \right. \\ \left. \left. \left. (0.0258y_1^2 + 0.0254y_2^2 - 4.1914 \times 10^{-7}y_1y_3 + 0.0258y_3^2) \right. \right. \right. \\ \left. \left. \left. - \frac{128}{9}Cy_3^2 \right\} \text{Exp}\left[-\frac{(y_1^2 + y_2^2 + 2y_3^2)}{2d^2}\right] - b_s k_f (ay_1^2 + ey_1y_2 + ky_1y_3 \right. \right. \\ \left. \left. + by_2^2 + hy_2y_3 + cy_3^2) \right] \text{intx} \times \text{intz} + \int_{-\infty}^{\infty} dz_1 dz_2 dz_3 \left\{ \left[-\frac{8}{6m} \right. \right. \right. \\ \left. \left. \left. (0.0258z_1^2 + 0.0254z_2^2 + 5.1396 \times 10^{-6}z_1z_3 + 0.0258z_3^2) - \frac{128}{9}Cz_3^2 \right\} \right. \right. \\ \left. \left. \text{Exp}\left[-\frac{(z_1^2 + z_2^2 + 2z_3^2)}{2d^2}\right] - b_s k_f (az_1^2 + fz_1z_2 + lz_1z_3 + bz_2^2 + iz_2z_3 + cz_3^2) \right. \right. \\ \left. \left. + \iota Pz_2 \sin\theta \right] \text{intx} \times \text{inty} \right]. \quad (26)$$

Here $\text{intx} = \int_{-\infty}^{\infty} dx_1 dx_2 dx_3 \text{Exp}\left[-\frac{(x_1^2 + x_2^2 + 2x_3^2)}{2d^2}\right] - b_s k_f (ax_1^2 + dx_1x_2 + jx_1x_3 + bx_2^2 + gx_2x_3 + cx_3^2) + \iota P(x_1 + x_2 \cos\theta)$, $\text{inty} = \int_{-\infty}^{\infty} dy_1 dy_2 dy_3 \text{Exp}\left[-\frac{(y_1^2 + y_2^2 + 2y_3^2)}{2d^2}\right] - b_s k_f (ay_1^2 + ey_1y_2 + ky_1y_3 + by_2^2 + hy_2y_3 + cy_3^2)$

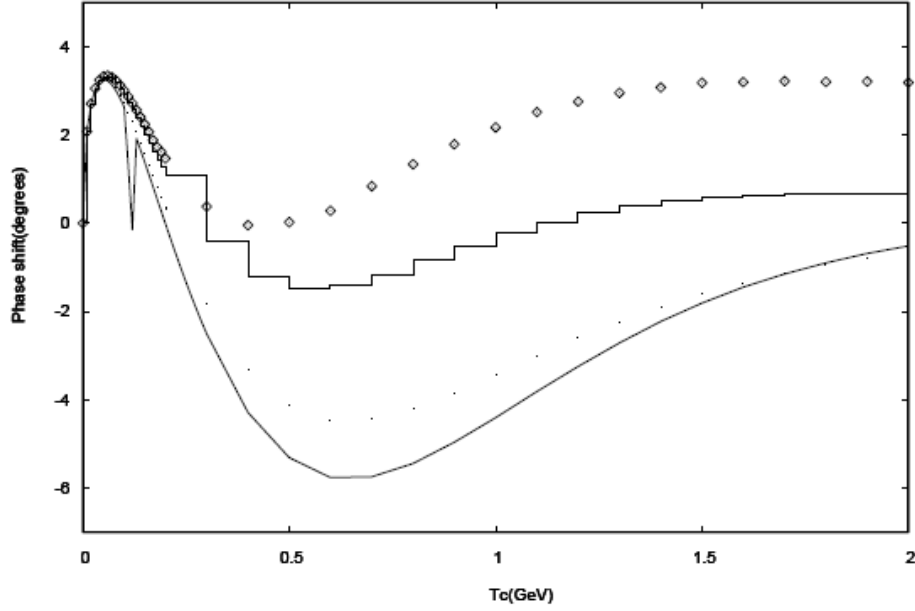


Figure 1: Comparison of phase shifts for different values of θ using S in f with $k_f = 0.57$. The graph with points only is for $\theta = 0$, with steps for $\theta = \frac{\pi}{6}$, with dots only for $\theta = \frac{\pi}{3}$ and with lines is for $\theta = \frac{\pi}{2}$.

and $intz = \int_{-\infty}^{\infty} dz_1 dz_2 dz_3 \text{Exp}[-\frac{(z_1^2 + z_2^2 + 2z_3^2)}{2a^2} - b_s k_f (a z_1^2 + f z_1 z_2 + l z_1 z_3 + b z_2^2 + i z_2 z_3 + c z_3^2) + \iota P z_2 \text{Sin}\theta]$. For this choice of S , we also calculated the phase shifts that are reported in the next section.

By treating eq.(18) in the same fashion as that of eq.(15) and using the Born approximation

$$\chi_1(\mathbf{R}_1) = \sqrt{\frac{2}{\pi}} \text{Exp}(\iota \mathbf{P}_1 \cdot \mathbf{R}_1) \quad (27)$$

it was checked that the results for phase shifts remain same. Actually eq.(18) and eq.(15) become identical if we interchange \mathbf{R}_1 and \mathbf{R}_2 .

5 Results and Conclusion

Fig.1 shows our results, with k_f defined by eq.(11) taken as 0.57, for the phase shifts for a selection of center of mass kinetic energies for different angles between \mathbf{P}_1 and \mathbf{P}_2 ; we have joined many points for clarity. These graphs indicates that for the kinetic energy above 0.2GeV the scattering angle has large effect on phase shifts, indicating a true gluonic field effect. That is, by increasing the scattering angle the phase shifts become large.

We noted that a faster convergence of the nine-dimensional integration (see eq.(23)) for larger kinetic energy values was possible for smaller values of the parameter k_f ; for a decrease in k_f of 0.1 the CPU time reduced at least three times to that for the previous value. This allowed us to get phase shifts for a larger set of kinetic energies using a smaller value of $k_f = 0.5$ considered in ref.[9]; the resulting more smooth phase shift graphs are shown in Fig.2. For comparing effects of the best lattice based non-separable f with other crude forms previously used, we show in the following Fig.3 the average of these $k_f = 0.5$ phase shifts over our selection of angle θ values together with the corresponding phase shifts for other forms of f i.e. exponent in f being proportional to S_a , $\sum_{i < j} r_{ij}^2$ and zero; the phase shifts were found to be independent of the angle θ for all these older forms of f and hence there was no need to take any angle-average for these other forms. This figure shows that in comparison to $k_f = 0$ (sum of two body potential model) we get relatively very small coupling with S , S_a and Gaussian form in f . So there are less chances of making a bound state with modifications in sum of two body approach i.e. the inclusion of gluonic field effects significantly decrease coupling between two mesons in a $q^2 \bar{q}^2$ system. Phase shifts are much less than 1 radian which indicates the validity of Born approximation. The phase shifts we

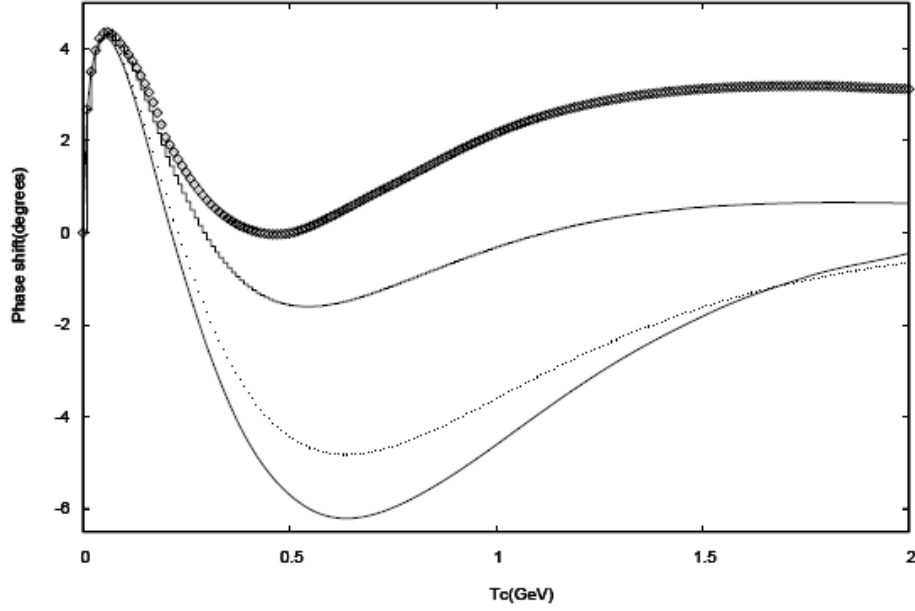


Figure 2: Comparison of phase shifts for different values of θ using S in f with $k_f = 0.5$. Choice of curve shapes is same as in fig 1.

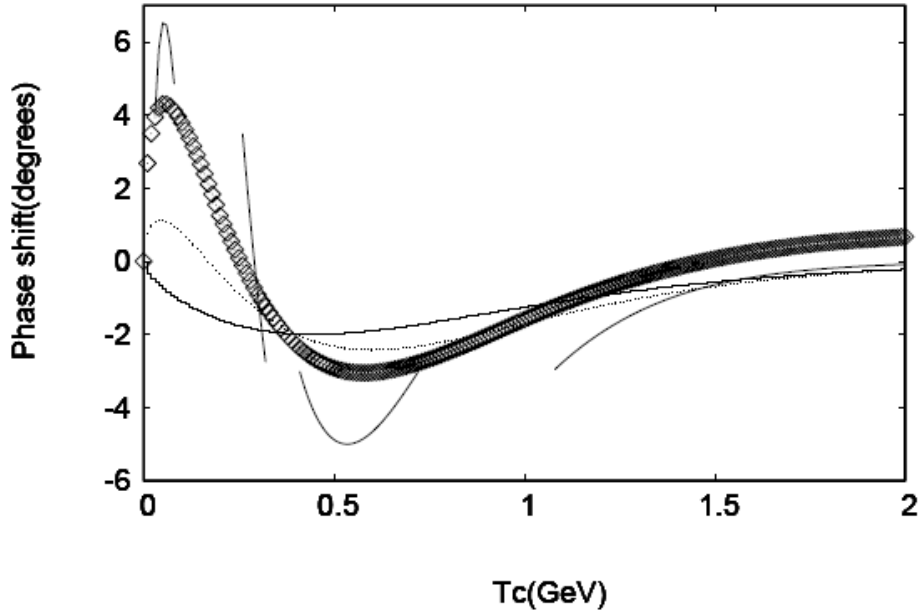


Figure 3: Comparison of different forms of f . Graph with lines only corresponds to $k_f = 0$, upper peak corresponds to actual data minus 28 and lower peak corresponds to actual data plus 5. Graph with dots corresponds to S_a in f . Graph with steps corresponds to gaussian form of f for $k_f = 0.075$ as defined by eq.(12). Graph with points corresponds to average of phase shifts for different values of angle θ for S in f with $k_f = 0.5$ defined by eq.(11).

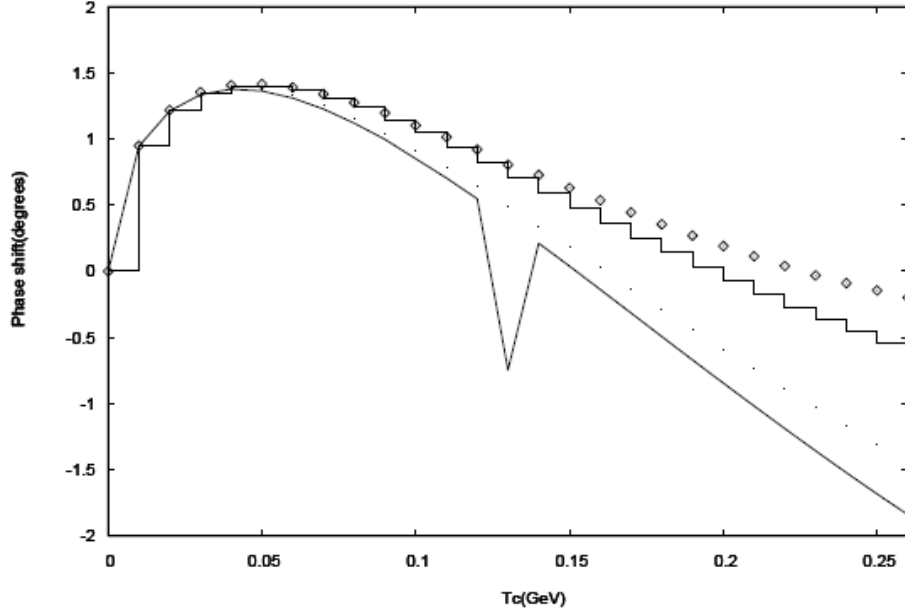


Figure 4: Comparison of phase shifts for different values of θ using S in f with $k_f = 0.8$. Choice of curve shapes is same as in fig 1.

get are lesser than reported by others who have used Born approximation [1] but not used f factor in off-diagonal terms.

It is to be noted that the S_a form also does not result in any angle dependence, although in contrast to the $f = 1$ and Gaussian form there is apparently no a priori reason to expect such an angle independence for the use of S_a . This may be because S_a is almost Gaussian with a little mixture of x_1x_3 and z_1z_3 terms (see eq.(14) and the parameter values reported just below it) or because S_a can be converted to a Gaussian form by a completing of squares. As for a comparison of the S_a phase shifts with the angle-average of the S phase shifts, it can be pointed out that the height of phase shift with S_a became less than that with original S but the shape remains identical. Perhaps this indicates that S_a simulates well some variations resulting from the original S form. In Fig.3 if we compare graph of Gaussian form with that of S in f we find that as compared to Gaussian form the graph of other forms is closer to $k_f = 0$, though the height of graph with $k_f = 0$ is still very large as compared to both Gaussian form of f and that of S in f .

A value of $k_f = 1.0$ higher than (0.5 and 0.57) that we have used in our calculations reported so far has been mentioned in ref. [19]. Although this work analyzes a relatively limited collection of geometries (only squares and tilted rectangles), we have tried to see effects of using a higher k_f . The numerical problems for large k_f implied in the above mentioned numerical convenience for smaller k_f did not allow us to get results for $k_f=1$ in a manageable time even for $T_c = 0.1\text{GeV}$. The best we could do was to do a number of calculations for $k_f = 0.8$; the resulting phase shifts from these are shown in Fig.4. Based on Fig.4, we expect that for higher values of k_f the results will remain qualitatively same and do not expect any new feature to emerge for $k_f = 1$.

References

- [1] T. Barnes and E.S. Swanson, Phys.Rev. **D46** 131-159 (1992).
- [2] A. M. Green, C. Michael, J.E. Paton, Nucl.Phys. **A554** 701-720 (1993).
- [3] B. Masud, J.Paton, A.M. Green and G.Q. Liu, Nucl.phys. **A528** 477-512 (1991).
- [4] C. Alexandrou, T. Karapiperis, O. Morimatsu, Nucl.Phys. **A518** 723-751 (1990).
- [5] J. Weinstein and N. Isgur, Phys.Rev.**D27** 588-599 (1983).

- [6] A. M. Green, J. Koponen and P. Pennanen, Phys.Rev. **D61**, 014014, (1999).
- [7] B. Masud , Phys. Rev. **D50**, 6783-6803 (1994).
- [8] H. Matsuoka and D. Sivers, Phys.Rev. **D33** 1441-1449 (1986).
- [9] A.M. Green and P. Pennanen, Phys.Rev. **C57** 3384-3391 (1998).
- [10] B. Silvestre-Brac and C. Semay, Z.Phys. **C57** 273-282 (1993).
- [11] E.S. Swanson, Ann.Phys. (N.Y.) 220,73 (1992).
- [12] John Archibald Wheeler, Phys.Rev. **52** 1083 (1937).
- [13] M. Imran Jamil and Bilal Masud, in progress.
- [14] J. Weinstein and N. Isgur, Phys.Rev. **D41** 2236 (1990).
- [15] N. Isgur and J. Paton, Phys.Rev. **D31** 2910 (1985).
- [16] M. Teper, Phys. Lett. **B397**, 223 (1997).
- [17] S. Furui, A.M. Green and B. Masud, Nucl.Phys **A582** 682-696 (1995).
- [18] D. Ahmad and B. Masud, in progress.
- [19] Petrus Pennanen, Phys.Rev. **D55** 3958 (1997).